

## Infochemistry: Encoding Information as Optical Pulses Using Droplets in a Microfluidic Device

Michinao Hashimoto,<sup>†</sup> Ji Feng,<sup>†</sup> Roger L. York,<sup>†</sup> Audrey K. Ellerbee,<sup>†</sup>  
Greg Morrison,<sup>‡</sup> Samuel W. Thomas III,<sup>†</sup> L. Mahadevan,<sup>‡</sup> and  
George M. Whitesides<sup>\*†</sup>

*Department of Chemistry and Chemical Biology, 12 Oxford Street, and School of Engineering and Applied Sciences, 29 Oxford Street, Harvard University, Cambridge, Massachusetts 02138*

Received June 11, 2009; E-mail: gwhitesides@gmwhgroup.harvard.edu

**Abstract:** This article describes a new procedure for generating and transmitting a message—a sequence of optical pulses—by aligning a mask (an opaque sheet containing transparent “windows”) below a microfluidic channel in which flows an opaque continuous fluid containing transparent droplets. The optical mask encodes the message as a unique sequence of windows that can transmit or block light; the flow of transparent droplets in the channel converts this message into a sequence of optical pulses. The properties of the windows on the mask (e.g., their size, wavelength of transmittance, orientation of polarization) determine the information carried in these optical pulses (e.g., intensity, color, polarization). The structure of a transmitted signal depends on the number and spacing of droplets in the channel. Fourier transformation can deconvolve superimposed signals created by the flow of multiple droplets into the message that a single droplet would transmit. The research described in this contribution explores a new field at the intersection of chemistry, materials science, and information technology: *infochemistry*.

### Introduction

This article describes a method of generating and transmitting information as a sequence of optical pulses, using a simple microfluidic device. A pattern of transparent windows in an otherwise opaque optical mask encodes the information (Figure 1). The fluids used in the device comprise an opaque continuous phase (water containing black ink) and transparent droplets (perfluoromethyldecalin, PFMD). The channel transmits light incident perpendicular to the mask only when a droplet flows underneath a window; alignment of a window and a droplet allows the device to generate a pulse of light. The device is, in effect, a series of optical shutters that open and close as the transparent droplets of PFMD pass between transparent windows and the source of light. The system can transmit non-binary (base  $N$  greater than 2) information using a scheme in which the optical pulses differ in the intensity, color, and polarization of the transmitted light. This ability to generate and transmit information (a “message”) with multistate pulses of light presents interesting problems in fidelity of transmission, cost, information/entropy, and error detection/correction that are less well explored than those in simple binary. We also demonstrate that operating the device in a mode in which multiple droplets move simultaneously in the microfluidic channel can serve as a weak form of encryption.

We refer to processes that transmit information using chemical (here, fluidic and optical) strategies, without electricity, as *chemical communication*. Such processes are a component of the broader subject of “infochemistry”—the intersection of chemistry, materials science, and information technology. Other

examples of chemical communication that we are currently exploring include infofuses, droplet lasers, and oscillating flames.<sup>1</sup> The transfer of information requires (at least) three major steps: generation, transmission, and detection. The vast majority of communication technologies use electromagnetic radiation and/or electrical potential, with photons or electrons as the working fluid.<sup>2,3</sup> Biological systems communicate messages using chemicals (for example, mRNA for transmission of information from the DNA to the ribosome), and chemicals are integral to a wide range of analog communication systems using hormones, pheromones, and other signaling molecules.<sup>4–6</sup> There are a number of reports of molecules that process digital information by using reactants (chemical, electrical, or optical) as inputs and the observable properties of the products of chemical reactions or transformations (such as a change in absorbance or fluorescence) as outputs. Such systems of so-called “molecular logic”<sup>7</sup> are, however, slow and difficult or impossible to integrate into a system comprising multiple parts in which the output of one device controls the function of another (as is required in almost all useful logic operations or circuits).

- (1) Thomas, S. W.; Chiechi, R. C.; LaFratta, C. N.; Webb, M. R.; Lee, A.; Wiley, B. J.; Zakin, M. R.; Walt, D. R.; Whitesides, G. M. *Proc. Natl. Acad. Sci. U.S.A.* **2009**, *106*, 9147–9150.
- (2) Feynman, R. P.; Hey, A.; Hey, T.; Allen, R. W. *Feynman Lectures on Computation*, 1st ed.; Westview Press: Boulder, CO, 2000.
- (3) Baeyer, H. C. v. *Information*, 1st ed.; Harvard University Press: Cambridge, MA, 2004.
- (4) Nishizuka, Y. *Science* **1986**, *233*, 305–312.
- (5) Hershko, A.; Ciechanover, A. *Annu. Rev. Biochem.* **1998**, *67*, 425–425.
- (6) Locasale, J. *BMC Syst. Biol.* **2008**, *2*, 108–108.
- (7) Szaciłowski, K. *Chem. Rev.* **2008**, *108*, 3481–3548.

<sup>†</sup> Department of Chemistry and Chemical Biology.

<sup>‡</sup> School of Engineering and Applied Sciences.

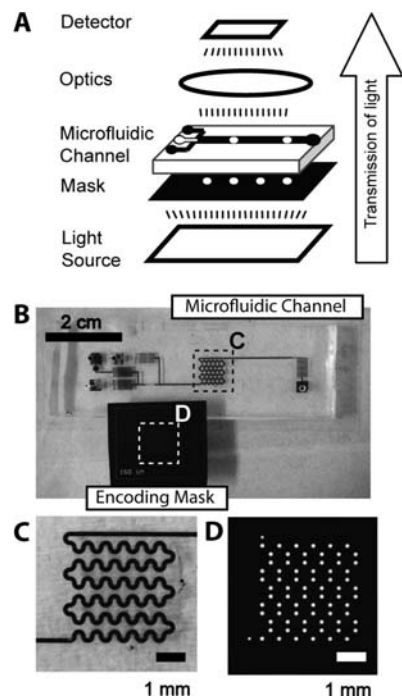


**Figure 1.** Schematic illustration of the architecture of the device used to generate optical pulses. (A) The setup of the device comprises five components: a source of light, an optical mask, a microfluidic droplet generator and fluidic channel, light-collecting optics, and a detector of light. (B) An optical micrograph of the entire microfluidic device and the mask, and magnification of (C) the coding region (filled with black ink) and (D) the encoding mask. The encoding mask is placed underneath the microfluidic device during the experiment.

Infochemical strategies for communicating information have five characteristics that differentiate them from existing methods of communication: (i) They can function even when electricity is not accessible or is only available in limited supply. (ii) They release energy from chemical reactions (i.e., combustion of hydrocarbons) with  $10\text{--}100\times$  higher volumetric energy densities than do batteries. (iii) They can encode information using orthogonal chemical and physical properties (e.g., intensity, wavelength, polarization of light). (iv) They can integrate chemical sensing with transmission of information about their environment. (v) They can operate in environments where electronic systems might fail (e.g., underwater, inside the body, in strong electromagnetic fields).

Microfluidic technologies offer precise control over the flow of multiphase fluids. Multiple immiscible phases—bubbles and droplets generated in microfluidic systems such as flow-focusing (FF) junctions<sup>8,9</sup> and T-junctions<sup>10</sup>—are useful in a range of chemical applications such as analytical studies of kinetics, syntheses of particles and drugs, encapsulation, delivery of reagents, mixing, generation of modulated light, and crystallization of proteins.<sup>11–14</sup> FF junctions also make it possible to form emulsions with very narrow size distributions (polydis-

persity  $<2\%$ ) at high frequency ( $\sim 100$  kHz for the formation of bubbles, and  $\sim 10$  kHz for the formation of droplets in PDMS devices).<sup>15,16</sup> For a given set of flow parameters (i.e., rates of flows and/or pressure of gas applied to the system), the frequency of droplet generation is constant. The patterns formed by bubbles or droplets range from simple periodic patterns to patterns that are almost artistically complex.<sup>17,18</sup> Two previous studies have suggested the idea of using bubble trains in microfluidic systems for communication. These reports include methods of encrypting and decrypting information that trains of droplets carry by using nonlinearities to generate aperiodic, complex sequences of bubbles<sup>19</sup> and methods of using bubbles for elementary logic functions.<sup>20</sup>

The objective of this research is to explore one possible strategy—a microfluidic device that transmits a message encoded in an optical mask as pulses of light—for chemical communication: that is, to prototype a system that would allow us to estimate the bit rate, fidelity, range, information density, and other characteristics of a droplet-based system for transmission of information. This paper describes three specific parts of our explorations: (i) We generate a sequence of pulses of light using a simple mask design (circular windows with a single area) to demonstrate the principle of this method. (ii) We extend this procedure to encode signals using a system with base  $N > 2$  (i.e., more than two states) using (a) windows of four different diameters with relative areas 0, 1/3, 2/3, and 1, (b) wavelength-selective filtering of light, and (c) polarization-selective filtering of light. (iii) We superimpose signals generated by multiple droplets present in the coding channel simultaneously and recover the original message from the superposed signal by Fourier transform. We explicitly restrict our attention to considerations of *encoding* and *transmitting* information and assume that conventional, electrically based optical systems of telescopes, spectrometers, and polarization detectors will receive—that is, detect and process—the optical information.

## Experimental Design

**Architecture of the Device.** Figure 1A illustrates the architecture of the device, and Figure 1B shows optical micrographs of the mask and actual device. The device used a source of white light and an opaque mask containing a set of windows that transmit light; the position, area, and wavelength- and polarization-dependent transmissivity of a given window determined the state of the light transmitted through that window. The mask was aligned with a microfluidic channel; the flow of an opaque continuous phase transported suspended, transparent droplets. The volume of the droplets approximately filled the channel (i.e., the droplets appear plug-shaped); a droplet passing in front of a window generated a pulse of light ( $\sim 5\text{--}50$  ms of half-width at half-maximum). We detected the light that passed through the optical mask with a fast video camera (1000 frames/s) or a spectrometer. Figure 2A illustrates the alignment of a

- (8) Gañán-Calvo, A. M.; Górrillo, J. M. *Phys. Rev. Lett.* **2001**, *87*, 274501.  
 (9) Anna, S. L.; Bontoux, N.; Stone, H. A. *Appl. Phys. Lett.* **2003**, *82*, 364–366.  
 (10) Thorsen, T.; Roberts, R. W.; Arnold, F. H.; Quake, S. R. *Phys. Rev. Lett.* **2001**, *86*, 4163–4166.  
 (11) Psaltis, D.; Quake, S. R.; Yang, C. *Nature* **2006**, *442*, 381–386.  
 (12) Song, H.; Chen, D. L.; Ismagilov, R. F. *Angew. Chem., Int. Ed.* **2006**, *45*, 7336–7356.  
 (13) Huebner, A.; Sharma, S.; Srisa-Art, M.; Hollfelder, F.; Edel, J. B.; Demello, A. J. *Lab Chip* **2008**, *8*, 1244–1254.

- (14) Shah, R. K.; Shum, H. C.; Rowat, A. C.; Lee, D.; Agresti, J. J.; Utada, A. S.; Chu, L.-Y.; Kim, J.-W.; Fernandez-Nieves, A.; Martinez, C. J.; Weitz, D. A. *Mater. Today* **2008**, *11*, 18–27.  
 (15) Garstecki, P.; Gitlin, I.; DiLuzio, W.; Whitesides, G. M.; Kumacheva, E.; Stone, H. A. *Appl. Phys. Lett.* **2004**, *85*, 2649–2651.  
 (16) Joanicot, M.; Ajdari, A. *Science* **2005**, *309*, 887–888.  
 (17) Garstecki, P.; Whitesides, G. M. *Phys. Rev. Lett.* **2006**, *97*, 024503.  
 (18) Hashimoto, M.; Garstecki, P.; Stone, H. A.; Whitesides, G. M. *Soft Matter* **2008**, *4*, 1403–1413.  
 (19) Fuerstman, M. J.; Garstecki, P.; Whitesides, G. M. *Science* **2007**, *315*, 828–832.  
 (20) Prakash, M.; Gershenfeld, N. *Science* **2007**, *315*, 832–835.

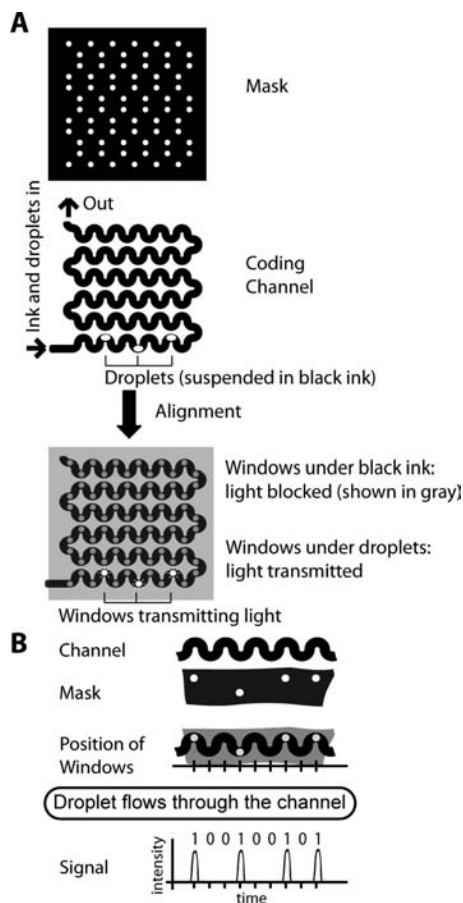


**Figure 2.** (A) Coding region: the design of a transparency-based mask, consisting of a series of open and closed windows, aligned with a modified serpentine microfluidic channel. The transmission characteristics of each window code for the message to be transmitted. Light passes through the device when a transparent droplet flows above a window. (B) Position of windows (either open or closed) are located at each turn of the coding channel.

microfluidic channel (the *coding channel*) and an optical mask. The mask shown here is the simplest possible configuration of the system: the presence or absence of circular windows of uniform diameter ( $150\ \mu\text{m}$ ) encodes binary information. When a transparent droplet passed over a window, the device transmitted a pulse of light (Figure 2A; white spots on the drawing). The fluids flowing through the device translated the sequence of windows in space on the mask into a series of optical pulses in time.

A sequence of semicircles oriented to provide a constant turn radius for the droplet composed the fluidic channel (Figure 2B); this design maximized the number of windows placed on a rectangular array while keeping the bit rate (the inverse of the time for a droplet to travel between two adjacent windows) roughly constant over the entire coding region. In contrast, a regular serpentine-shaped fluidic channel (i.e., a channel comprising straight sections of channel connected by semicircles) would produce a nonconstant bit rate—leading to nonequal separation between optical pulses—at the turns, even when adjacent windows *on the mask* were spaced equally. Variations in the velocity of the droplet traversing the turn in the channel, relative to its velocity while traversing in a straight region of channel, would cause this variation in bit rate. While judicious spacing of the windows on the mask could, in principle, compensate for this nonuniformity in the velocity, the use of

multiple semicircles offered a simple solution to ensure constant separation in time between the optical signals from adjacent windows spaced uniformly for the entire coding region.

**Choice of Fluids and Other Materials.** For most experiments, we used aqueous black ink as the continuous phase and perfluoromethyldecalin (PFMD, transparent to visible light) as the dispersed (droplet) phase. We chose these materials for two reasons: (i) both fluids are readily available commercially, and (ii) both fluids are compatible with a polydimethylsiloxane (PDMS) device (i.e., they do not swell PDMS).<sup>21</sup> The microfluidic system was prepared by sealing a system of channels molded in PDMS to a flat glass slide by plasma oxidation followed by contact.<sup>22</sup> All materials used to fabricate the channel system were also transparent to the wavelengths of light that we used throughout the experiments.

**Definition of Bit Rate.** The design and operation of the device determine and control two characteristics important for communication of messages: the bit rate and the base ( $N$ ) of the number system used for encoding information (e.g.,  $N = 2$  for binary;  $N = 10$  for decimal). A *bit* (or binary digit) is the smallest unit of information that can be used to convey a unique signal or message state; a bit takes two possible values, 0 or 1. Here, we encoded a message using a fundamental unit that can take more than two possible values<sup>23–25</sup> due to distinguishable properties of light (i.e., intensity, wavelength, and polarization).<sup>26–29</sup> Each unit of information (here, a window) can take  $N$  possible values, where  $N$  is the base of the system; the number of unique values that an individual unit can possess defines the *encoding base* of the system. For example, a base-4 system implies that each unit can take on any of four possible values. Essentially all of modern information technology is based on binary or variants of binary (e.g., octal or hexadecimal), because algorithms for error-checking are most developed for binary systems and because operations such as latching make binary intrinsically low in error rates.

In this paper, a *window* on the mask—in registration with the channel—determines a unique state for the information transmitted (Figure 2B). Each window is unique and must be spaced sufficiently (with respect to the length of droplets) apart from neighboring windows to avoid overlap of signal with them. The minimum number of windows needed to encode a unique character within a given set of characters depends on the encoding base and the number of characters in the set, and is given by  $\text{ceil}(\log_N(A))$ , where  $N$  is the encoding base,  $A$  is the number of characters in the set, and the  $\text{ceil}()$  function rounds

- (21) A change in channel geometry from swelling of the PDMS would affect the length (and height) of the droplets, leading to optical pulses with different widths. In particular, if the swelling of the PDMS device was time-dependent, the device would not generate consistent signals over extended periods of time.
- (22) McDonald, J. C.; Duffy, D. C.; Anderson, J. R.; Chiu, D. T.; Wu, H.; Schueller, O. J. A.; Whitesides, G. M. *Electrophoresis* **2000**, *21*, 27–40.
- (23) Hurst, S. L. *IEEE Trans. Comput.* **1984**, *33*, 1160–1179.
- (24) Cignoli, R. L.; d'Ottaviano, I. M.; Mundici, D. *Algebraic Foundations of Many-Valued Reasoning*, 1st ed.; Springer: New York, 1999.
- (25) Gottwald, S. *A Treatise on Many-Valued Logics*, 1st ed.; Research Studies Press: Hertfordshire, UK, 2001.
- (26) Alasfar, S.; Ishikawa, M.; Kawata, Y.; Egami, C.; Sugihara, O.; Okamoto, N.; Tsuchimori, M.; Watanabe, O. *Appl. Opt.* **1999**, *38*, 6201–6204.
- (27) Ditlbacher, H.; Lamprecht, B.; Leitner, A.; Aussenegg, F. R. *Opt. Lett.* **2000**, *25*, 563–565.
- (28) Pham, H. H.; Gourevich, I.; Oh, J. K.; Jonkman, J. E. N.; Kumacheva, E. *Adv. Mater.* **2004**, *16*, 516–520.
- (29) Li, X.; Chon, J. W. M.; Wu, S.; Evans, R. A.; Gu, M. *Opt. Lett.* **2007**, *32*, 277–279.

up to the nearest whole number. For example, describing one unique character from a set of 56 alphanumeric characters (e.g., a set comprising 10 numerals, 26 letters, and 20 punctuation marks) using a binary encoding base ( $N = 2$ ) requires six units (or bits, since we are concerned with binary encoding in this example), because  $\text{ceil}(\log_2(56)) = 6$  (i.e.,  $2^5 < 56 < 2^6$ ). In fact, six binary bits can, in principle, encode up to  $2^6 = 64$  unique characters.

Windows with different areas change the intensity of the optical signal. In general, the use of windows of  $m$  different areas corresponds to a base- $(m + 1)$  representation (the closed window also provides one unique state, and thus yields  $m + 1$  different signals). Number systems with larger values of  $N$  can encode more information in each unit than those with lower values, but are more susceptible to errors of a number of types and are generally more complicated to implement in reliable hardware. Systems with large values of  $N$  may, however, interface more easily with chemistry (which is intrinsically an analog or continuous system) than do binary systems.

To illustrate the economy with which systems based on values of  $N$  greater than 2 can operate, consider a system with  $N = 4$ . If we use windows of three different areas ( $N = 4$ ; closed = 0, open-small =  $1/3$ , open-medium =  $2/3$ , and open-large = 1), three units, or windows, can represent a set of 56 alphanumeric characters (i.e.,  $4^2 < 56 < 4^3$ ). Base- $N$  encoding can be accomplished using multiple states of intensity but also (and perhaps more relevant to chemistry) using other properties, such as the polarization state and color of transmitted light.

The linear speed of a droplet along the channel and the distance between adjacent windows determine the *bit rate* ( $f_b$ ). We delivered the fluids to the channel at a constant *volumetric* rate of flow; the velocity of a volume of fluid *in the channel* (which is proportional to the velocity of a droplet) is therefore the volumetric rate of flow divided by the cross-sectional area of the channel. Equation 1 describes the bit rate  $f_b$ , where  $v$  is the velocity of a unit volume of fluid,  $Q$  is the volumetric rate of the flow,  $w$  and  $h$  are the width and height of the channel cross-section, and  $d$  is the separation between windows on the mask. The bit rates in systems with a base of  $N$  are higher than the bit rate of the binary system by the factor of  $\log_2 N$ . (For example, the bit rate of a system with  $N = 4$  is twice (i.e.,  $\log_2 4 = 2$ ) as high as that in a binary system.) The amount of information that each window on the mask possesses increases as  $N$  increases. Changing any of these physical variables, flow parameters, or the base number changes the bit rate.

$$f_b = \left(\frac{v}{d}\right) \log_2 N = \left(\frac{Q}{whd}\right) \log_2 N \quad (1)$$

## Results and Discussion

**Proof of Principle of Operation of a Device.** Figure 1A illustrates the general architecture of the system. We used the light source and optics of an upright microscope to illuminate the device and a fast video camera to record the output signal. (This arrangement is obviously inappropriate for a system designed for a field use but allows us to explore the parameters relevant to the operation of the device.) The distance between the light source and coding device was 15 cm; the distance between the device and detector was 30 cm. First, we verified that the device functioned as expected, using the simplest possible design of the mask and structure of the train of droplets. (The structure of the train of droplets refers to the number and relative spacing of droplets present simultaneously in the

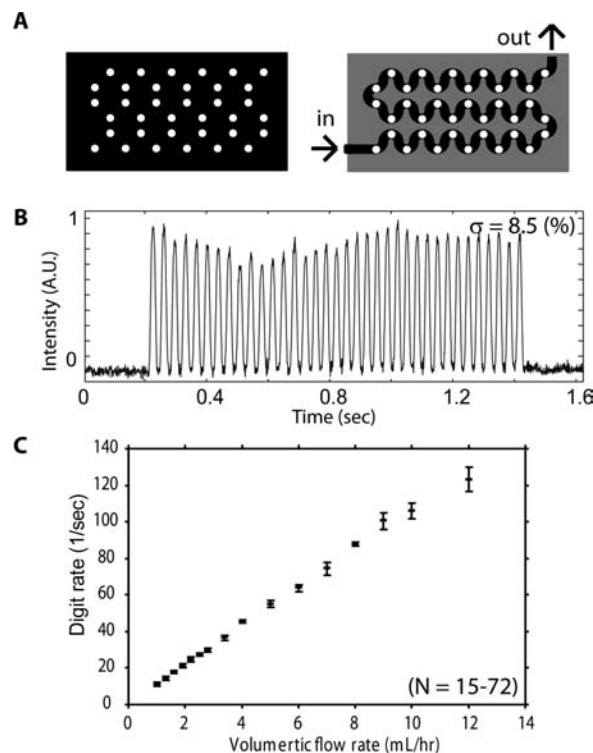


**Figure 3.** (A) Mask used for a proof-of-principle demonstration to test the optical output of the device upon proper alignment of the mask with the channel; all windows are open (i.e., 1's) and transmit light. (B) Pulses for the light signal generated by the mask illustrated in panel A. The standard deviation of the signal intensity was 8.5%; the signal-to-noise ratio (S/N) was 1/30. (C) Plot describing the relationship between the bit rate ( $f_b$ ) and the volumetric flow rate ( $Q$ ) applied to the system. The relationship was linear for the range of  $Q$  demonstrated (1–12 mL/h).

channel.) The mask had transparent windows in all possible positions (i.e., all bits represent '1'), and we delivered only one droplet to the coding region. Figure 3A shows the signals generated from the experiment and establishes the reproducibility of the signal (S), noise (N), and their ratio ( $S/N \approx 30$  in these experiments); all these parameters were important in understanding the limitations of multistate systems, although the S/N ratio was the most important. Equation 1 states that the bit rate is linearly proportional to the volumetric flow rate ( $Q$ ); we could tune the bit rate between 10 and 120 Hz by changing  $Q$  (Figure 3C). The upper limit of the bit rate was determined by the flow rate of the fluids at which the microfluidic device failed (i.e., the sealing between the PDMS slub and the glass substrate broke) due to internal pressure exerted by the flow of fluids.

**Qualitative Discussion of S/N Pertinent to the System.** The number of the states of windows that can be easily distinguished depends on the noise of the signal at the receiver (and ultimately—although we do not address this subject here—the methods used for error checking and correction). For the droplet shutter, an idealized setup (without bounds on the intensity from the light source) would have three primary sources of noise that contribute directly to the signal-to-noise ratio: (i) Imperfections in the areas of the windows in the shutter would alter the emitted intensity of light but would not alter the color, peak-to-peak distance, or polarization of the received signal. (ii) Fluctuations in the velocity of a droplet as it travels the coding channel would alter the time interval between peaks and could alter the intensities of transmitted light. (iii) Insufficient sampling rates of the detection device (i.e., a low-speed camera) might cause

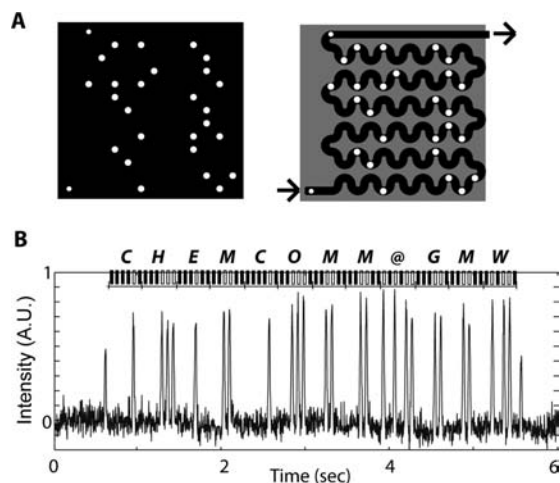


**Figure 4.** Transmission of a message using windows of a single size (base-2). (A) A mask and mask–channel alignment encoding for the message “CHEMCOMM@GMW”. (B) The detected optical signal. The message was decoded using the coding table (Figure S1A in the Supporting Information).

fluctuation of the detected intensity of light due to omission of the frame when the droplet and the window are fully aligned. Partial coverage of the window by the droplet does not pass light at maximum intensity from the window, and—depending on the area of the window, the length of the droplets, and the velocity of the droplets in the channel—the detection device might fail to collect the frames that show the full intensity of light from a given window. An understanding of the statistical behavior of these fluctuations will give insight into the conditional probability distribution function between the received and intended signals, from which the capacity of the channel can, in principle, be computed. A detailed analysis of the fluctuations due to each of these sources, as well as a simple estimate for the channel capacity of such a system, is reserved for a later publication.

### Single-Droplet Experiments

**Encoding a Message Using Windows of a Single Size.** We used a unique combination of six bits to encode each character from a set of 56 symbols (26 letters, 10 numbers, and 20 punctuation marks) using a sequence of circular windows with uniform area (Figure S1, Supporting Information). Figure 4A shows the mask that encoded a 12-character message—CHEMCOMM@GMW—that required 72 bits to translate. Figure 4B shows the corresponding time sequence of optical pulses that transmitted this message. The initial and final pulses with half intensity mark the beginning and end of the message. After the initial pulse in the message sequence was located, the optical pulses were mapped to a unique sequence of ‘0’s and ‘1’s (Figure 3C); we decoded the original message with the encoding table in Figure S1.

**Encoding a Message Using Windows of Multiple Sizes.** In order to increase  $N$  and the information transmitted per window, we used different areas of windows to generate optical pulses of multiple intensities. Figure 5A is a plot of the intensity of the pulses as a function of the area of the windows. We could not distinguish signals from windows with areas that differed in intensity by less than one-third. For example, we could not reliably distinguish the signal intensity generated by a full-sized window with a diameter of  $150\ \mu\text{m}$  (area =  $17\,700\ \mu\text{m}^2$ ) from that generated by windows that were 83% or 92% of the original

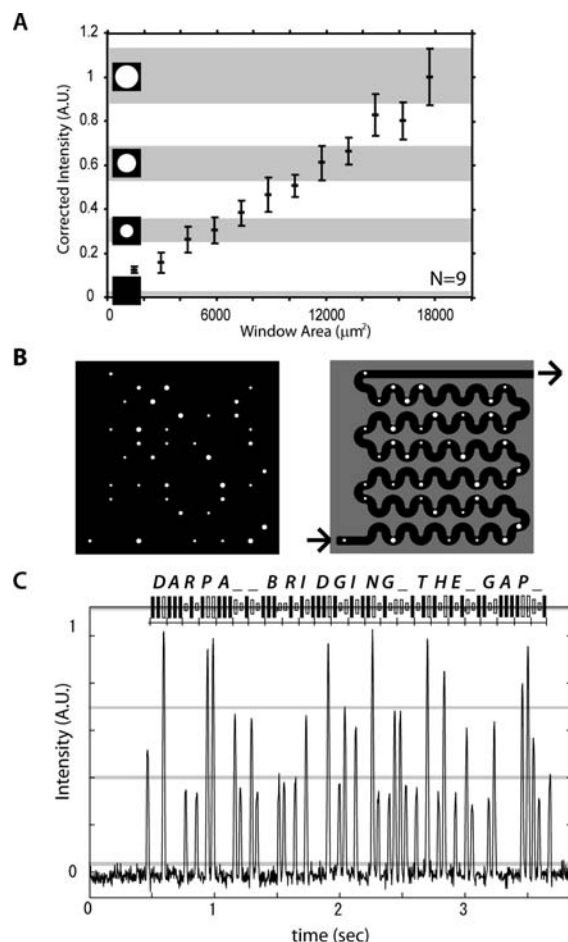


**Figure 5.** Transmission of a message using windows with different areas (base-4). (A) A plot describing the intensity of light with respect to the area of the window transmitting the light. The average intensity transmitted through the window of the largest area is set to 1. Windows of three sizes and a closed window produced distinguishable readouts of the intensity of signals (shaded gray). (B) Mask encoding the message “DARPA\_BRIDGING\_THE\_GAP\_” and schematic illustration of the alignment of the mask with coding channel. (C) The detected optical signal. Vertical lines are the upper threshold of the intensity of light transmitted for each size of window (i.e., relative areas of 0 (closed), 1/3, 2/3, and 1 (fully open)). The message was decoded using a coding table (Figure S1B in the Supporting Information).

area of the window. We used a base-4 system (the relative areas of circular windows were 1, 2/3, 1/3, and 0) to encode a message; the system was able to distinguish intensities transmitted from these windows (Figure 5A). We encoded the 24-character message: “DARPA\_BRIDGING\_THE\_GAP\_” (Figure 5B,C) using 72 windows. The base-4 representation required three windows to identify a unique character in the set of 56 characters and was twice as efficient in terms of the utilization of space on the mask as a base-2 representation (Figure S1).

**Encoding a Message Using Wavelength-Selective Filtration of Light.** Wavelength-selective filtration of broadband light provided an alternative way to increase  $N$ . By aligning color filters with each window, we could change the wavelengths of light transmitted through each window on the mask (albeit with a lower intensity of the transmitted signal than when the window had no filter).

We created simple optical filters by painting selected windows on the mask one of three different colors (blue, red, and orange). Filtering the light in this way decreased the S/N ratio by decreasing the absolute intensity of light; practically, it is

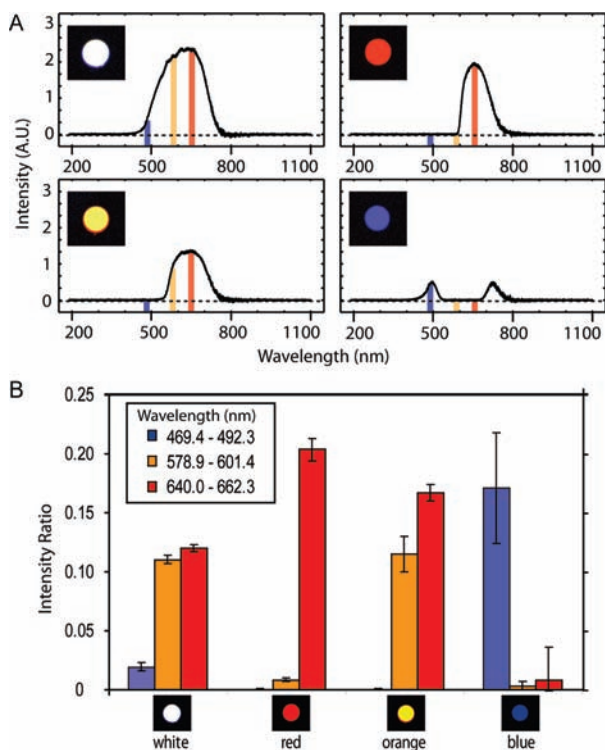


**Figure 6.** Resolving windows painted with filters of different colors. (A) Color spectra of light transmitting through a transparent window and windows painted with red, orange, and blue ink. The three colored bands marked in the spectra denote the wavelength ranges whose intensity ratios were used to aid in distinguishing the different windows. All windows were illuminated simultaneously by the same white light source. (B) Normalized intensity of the light received in each wavelength band for the various filters used.

important to choose the optical characteristics of the filter such that the noise of the system does not obscure the signal that the receiver detects. This system, which used these three colors in addition to white and black states (i.e., noncolored windows that are open or closed, transmitting or blocking all light, respectively), had a base of  $N = 5$ . Figure 6 shows the spectrum of broadband light transmitted through each filter (and the case for no filter). The plot shows the *normalized* intensity in three wavelength windows (i.e., the intensity of the light in the ranges of 469.4–492.3, 578.9–601.4, and 640.0–662.3 nm, relative to the intensity of the light integrated across the whole visible spectrum).

Figure 7A is an optical micrograph of the mask with colored windows and an illustration of its alignment with the channel. We demonstrated the encoding of signals using four different colors of light. The sequence of windows on the mask was “Red-Blue-Red-White-Orange-White-Blue-Orange-Orange-White”. Figure 7B shows the sequence of pulses we obtained; we could clearly distinguish signals from differently colored windows. We also demonstrated use of the device for a prolonged period of time: Figure 7C shows that our device generated the same signal stably over 80 min. The device transmitted more than 4800 indistinguishable copies of the signal during the course of the experiment.

**Encoding a Message Using Polarization-Selective Filtration of Light.** Polarization was another property of light that we explored to increase the base of the encoding number system. Linearly polarizing elements (here, a polarizing film) on each window of the mask (here, the white light is unpolarized) transmitted polarized light; we denote the polarization angle for

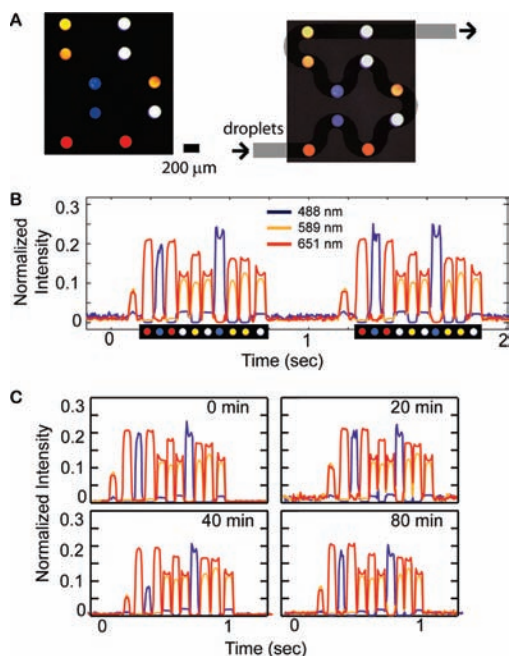


**Figure 7.** Encoding signals using a mask painted with three colors of ink. (A) An optical micrograph of a colored mask, and a schematic illustration showing alignment of the mask with an encoding channel. (B) A line spectrum describing the normalized intensities of signals observed at three windows of wavelengths for the mask shown in panel A. The optical signals of masks of four colors (i.e., transparent, blue, orange, and red) are distinguished clearly. (C) Continuous operation of the device. The device generates a reproducible signal over an extended period of time (80 min) and reliably encodes the original message.

each window of the mask as  $\theta_1$ . Polarized windows, in addition to the open and closed windows, constituted the full base for encoding in this scheme. To take advantage of this encoding scheme, it was necessary to use a detector sensitive to the polarization angle of incoming light. While it is possible to detect the polarization directly with polarization-sensitive detectors, manual addition of a linearly polarizing element (analyzer) in the light path just prior to the detector was a convenient way to detect polarized signals. We denoted the polarization angle of the analyzer as  $\theta_2$ . In this scheme, different polarization angles transmitted light with different *intensities*. Malus’s law (eq 2) describes the output intensity of light  $I$  after passing through a polarizer–analyzer sequence, where  $I_0$  is the intensity of light incident on the polarizer.<sup>30</sup>

$$\frac{I}{I_0} = \cos^2(\theta_2 - \theta_1) \quad (2)$$

Hence, changing the polarization angle  $\theta_2$  changes the transmitted intensity for a given window polarization  $\theta_1$ . Since the output of this system is intensity, the noise of the system makes it difficult to distinguish two polarization angles on the mask ( $\theta_1$ ) with similar values. While using more values of  $\theta_1$  to encode information increases the base  $N$ , it also increases the error rate.

Figure 8A illustrates the scheme of polarization-sensitive detection of light using this microfluidic device and two linear polarizers; we introduced unpolarized light to the device that passed through two polarizing elements before reaching the detector: one on the mask ( $\theta_1$ , mask) and one in front of the detector ( $\theta_2$ , analyzer). We set the polarizing angle of  $0^\circ$  parallel

(30) Hecht, E. *Optics*, 4th ed.; Addison Wesley: San Francisco, 2001.

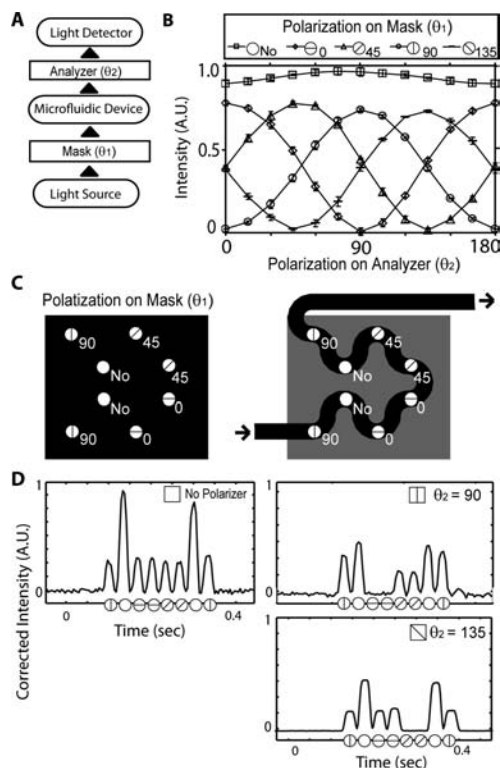


**Figure 8.** Encoding signals using a mask with windows containing linearly polarizing elements. (A) Flow chart describing the transmission of light in a polarization-sensitive detection scheme. We used two linearly polarizing elements in this experiment, one on the window of the mask ( $\theta_1$ ) and the other on the detector ( $\theta_2$ ). The polarization angle on the detector relative to that on the mask can be varied by rotating the analyzer. (B) Intensity of light transmitting through the two polarizers described in panel A. The polarization angle on the mask ( $\theta_1$ , here  $0^\circ$ ,  $45^\circ$ ,  $90^\circ$ , and  $135^\circ$ ) was fixed, while the orientation of the analyzer was varied from  $0^\circ$  to  $180^\circ$ . (C) A mask with polarizing windows and alignment with a coding channel. (D) Detected signals. Without the analyzer, all polarizing windows transmit signals with indistinguishable intensities (left). It is, however, possible to distinguish the polarization angle on each window ( $\theta_1$ ) when two signals are detected, one for each of two different orientations of the analyzer ( $\theta_2$ , here  $90^\circ$  and  $135^\circ$ ) (right).

to the direction of the flow in the microfluidic channel as it entered and exited the coding region. In general, the absolute values of the polarization angles  $\theta_1$  and  $\theta_2$  are arbitrary, because we needed only to determine the difference between them to distinguish different windows. Figure 8B shows the variation in the detected intensity of light for varying combinations of  $\theta_1$  and  $\theta_2$ . The intensity of the detected light varied as we changed the polarization of the analyzer; the periodicity of the variation of the intensity is  $180^\circ$ . In general, the measurement of intensity for only one polarization angle of the analyzer ( $\theta_2$ ) is not sufficient to distinguish the signals and infer uniquely the polarization of a given window on the mask ( $\theta_1$ ): for a given  $\theta_2$ , two different values of  $\theta_1$  satisfy Maull's law because of the symmetry of the cosine function (i.e.,  $\cos(x) = \cos(-x)$ ). Windows without a polarizer (denoted as "No") always yield the maximum intensity; the intensity for unpolarized windows is higher even than the intensity for the case where  $\theta_1 = \theta_2$ , because of the small loss of the intensity due to reflection from the interface of the polarizing film.

Figure 8C shows a schematic representation of a mask that we used to prove the principle of polarization-sensitive encoding; the mask contains windows with linear polarizers oriented at one of three different polarization angles ( $0^\circ$ ,  $45^\circ$ , and  $90^\circ$ ),

windows with no polarizer, and closed windows. We were able to distinguish signals transmitted through all five types of windows by the intensity of the light reaching the detector. Figure 8D shows the intensity of signals obtained with the mask in Figure 8C for different polarizations of the analyzer ( $\theta_2$ ). Without an analyzer, the intensity of detected signals cannot distinguish the polarization on the mask ( $\theta_1$ ): the intensity of light transmitted through polarized windows is equivalent regardless of the polarization angle, and only three levels of intensity—corresponding with open and not polarized, polarized, and closed windows—are distinguishable. With the analyzer in place, it was possible to establish each polarization on the mask ( $\theta_1$ ) (here,  $\theta_2 = 90^\circ$  and  $135^\circ$  are shown). The information from these two measurements was necessary to deduce the polarization on the mask. For example, the intensity of the fifth and the sixth signals from the measurement at  $\theta_2 = 90^\circ$  suggests that  $\theta_1$  is either  $45^\circ$  or  $135^\circ$ ; the intensity of the same peaks for the measurement at  $\theta_2 = 135^\circ$  is zero; it is therefore possible to deduce that  $\theta_2 = 45^\circ$  for these windows. The windows without a polarizer (i.e., the second and seventh windows) provide peaks of constant intensity regardless of the value of  $\theta_2$ —they are also the most intense. The intensity of the peaks from closed windows was always zero.

#### Multiplexing Signals Using Orthogonal Properties of Light.

This work has explored using intensity (via the size of windows), color (via colored windows), and polarization (via polarized windows) to encode information separately. If we were to look at all three parameters simultaneously—for example, three different areas of windows, four different colors, and four different polarization angles—it would be possible for each window to express 49 different states ( $3 \times 4 \times 4 + 1 = 49$ ) (including one state that represents a closed hole).

In our scheme, we inferred the polarization angle from the intensity of the transmitted light. In this setup, intensity and polarization did not represent orthogonal properties and could not be used simultaneously to increase  $N$ . It is possible, however, to decouple the measurement of the intensity of light from its polarization state by making two measurements for each window, each at different polarization angles (i.e., incorporate two different analyzers). The two measurements could be made simultaneously, by using two separate detectors and a beam splitter, or sequentially, using a single detector with a variable analyzer as shown in Figure 8D. In both cases, the polarization angles of the analyzers must be out of phase by some angle.<sup>31</sup> The major trade-offs of a system of this sort are increased cost and complexity due to the use of a second detector in the first case and a decrease in the rate of transmission of information by a factor of 2 in the second case.

#### Multiple-Droplet Experiments

It is possible to generate droplets moving through the channel over the mask at a rate such that multiple droplets of the same size transmit patterns of pulses of light at the same time. Although the resulting signal is more complex than the signal that single droplet transmits, it is possible to deconvolve it into the message that a single droplet would transmit. There are two reasons to consider such a procedure: (i) It would increase the bit rate of transmission of the device. Because multiple copies of the same message are being transmitted simultaneously, it

(31) To distinguish different values of  $\theta_1$ , the difference between the two polarization angles of the analyzer used for the detection (say,  $\theta_{2A}$  and  $\theta_{2B}$ ) must not be  $90^\circ$  ( $|\theta_{2A} - \theta_{2B}| \neq 90^\circ$ ).

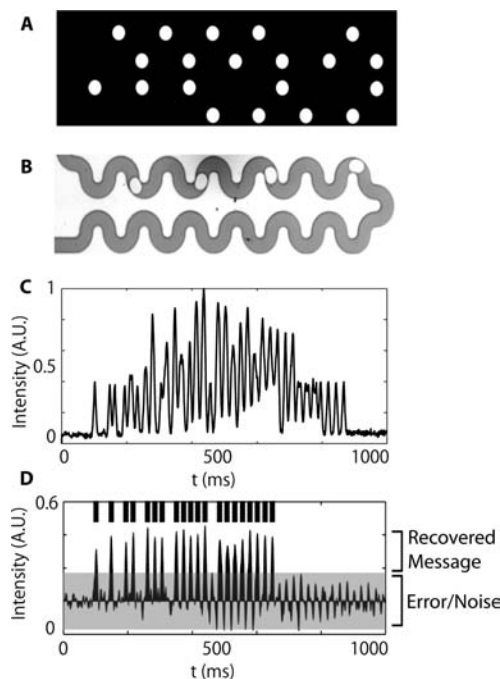


**Figure 9.** Recovery of a message from a multidroplet signal. (A) Design of the mask that encodes the following sequence of bits: (10101101110111101111110). (B) An optical micrograph of four droplets flowing through the coding region. (C) The signal generated using the mask in panel A for the four-droplet train observed in panel B is a superposition of four time-shifted, single-droplet signals. (D) The single-droplet signal recovered from the multidroplet signal by use of the Fourier transform matches the original message shown in panel A.

would increase the S/N ratio by decreasing the error rate and resolving dropped bits and other errors. (ii) It would provide a form of encryption, albeit a weak form. Because a straightforward mathematical procedure resolves the multiplexed, superimposed copies of the single message, it would be possible to resolve the message by performing trial-and-error scans over these variables. It would, however, require some computational capability to achieve this resolution. “Markers” in the message, such as color or polarized bits at known positions, could be used to indicate the number of, and the separation between, the droplets flowing through the channel and facilitate this process.

The signal obtained when multiple droplets are present in the channel is a superposition of the signals that a single droplet would generate, with discrete time delays; the spacing between the droplets and the number of droplets present in the channel determine these time delays. Provided that these time delays are known, the Fourier transform (FT) is an easy way to resolve the original, single-droplet message from the superimposed, multidroplet signal. In the following section, we discuss the underlying principles of the FT that enable deconvolution of the superimposed signal.

**Theory of Decomposing Superimposed Signals.** We denote by the time-dependent function  $g(t)$  the time profile of the pulse produced by a single droplet passing over a single, open window (i.e., a window whose ability to transmit light has not been modified by the addition of polarizers or color filters). We denote the original message  $\{A\}$  consisting of  $M$  units as  $\{A\} = \{A_1, A_2, \dots, A_M\}$ ; the number of units (or, equivalently, the number of windows on the mask)  $M$  is given by the product of the length of the character sequence to be transmitted and the base ( $N$ ). Equation 3 describes the signal produced by a single droplet

moving through the entire encoding region, where  $1/\tau$  ( $\text{s}^{-1}$ ) is the bit rate and  $A_j$  constitutes the optical transmission function (which may be wavelength- and polarization-dependent) of the corresponding units in the message. The bit rate is given by  $d^{-1}v$ , where  $d$  (cm) is the separation between windows and  $v$  (cm/s) is the rate of flow of a droplet.

$$f_1(t) = \sum_{j=0}^{M-1} A_j g(t - j\tau) \quad (3)$$

The FT of  $f_1(t)$  is given by eq 4, where  $\omega$  (rad/s) is the frequency-domain transform variable, otherwise known as the angular frequency.

$$\tilde{f}_1(\omega) = \int dt e^{-i\omega t} f_1(t) \quad (4)$$

Each droplet that enters the coding channel generates a signal that is a time-shifted version of  $f_1(t)$ ; the value of the time-shift depends on the time at which the droplet enters the channel (the channel entry time). Let  $\{\alpha\} = \{\alpha_0, \alpha_1, \dots, \alpha_{P-1}\}$  be the sequence of channel entry times associated with a series of  $P$  droplets that are in the coding region at the same time, all given relative to the channel entry time of the first droplet (i.e.,  $\alpha_0 = 0$ ). The signal  $f_p(t)$  acquired by the receiver is simply the sum of the signals generated by each individual droplet (eq 5). Because the FT is a linear transform, we can extract  $f_1(t)$ , the original signal that would be obtained in the case of a single droplet, from the overlapped signal.

$$f_p(t) = \sum_{k=0}^{P-1} f_1(t - \alpha_k) \quad (5)$$

The FT of  $f_p(t)$ , the superimposed signal, is found by applying the time-shifting property of the FT (eq 5); in this way, a time-shift in the time domain is converted to a multiplicative constant in the frequency domain (eqs 6 and 7).

$$\tilde{f}_p(\omega) = \tilde{f}_1(\omega) \sum_{k=0}^{P-1} e^{-i\omega\alpha_k} = \tilde{f}_1(\omega) \tilde{S}_N(\omega; \{\alpha_k\}) \quad (6)$$

$$\tilde{S}_N(\omega; \{\alpha_k\}) = \sum_{n=1}^{P-1} e^{-i\omega\alpha_n} \quad (7)$$

Here, we call the multiplication factor,  $\tilde{S}_N(\omega; \{\alpha_k\})$ , the *geometric structure factor*; the value of this term is determined by the number of droplets simultaneously present in the channel and the separation between droplets. The function  $\tilde{S}_N(\omega; \{\alpha_k\})$  is constant under constant rates of flow. Assuming that the number of, and the spacing between, droplets are known, recovery of  $f_1(t)$  can be accomplished by a three-step procedure: (i) calculate the FT of the overlapped signal, (ii) divide the result of the first step by  $\tilde{S}_N(\omega; \{\alpha_k\})$ , and (iii) take the inverse transform of the result of the second step.

This analysis is valid for any sequence  $\{\alpha\}$ , and  $\alpha_{k+1} - \alpha_k$  need not be constant (i.e., the separation between adjacent droplets may be different). Because the droplet generator we used in this experiment generates droplets at constant frequency, however, we worked with a system in which the separation between droplets was constant (i.e.,  $\alpha_{k+1} - \alpha_k = \alpha_1$ ). For a system with a single droplet,  $\{\alpha\} = \{0\}$ ; the signal we obtain leads directly to the information coded on the mask.



**Encoding a Message Using Windows of a Single Size.** Figure 9 shows the process for resolving the signal obtained from four droplets present in the channel simultaneously, using a mask with windows of a single area (a binary mask). The superimposed signal (Figure 9C) did not resemble the output for a single droplet. Fourier analysis recovered the original signal (Figure 9D). In the signal we recovered, the most intense peaks were higher than the noise by a factor of 2, and the recovered signal corresponded well with the original message. Fluctuations in the spacing between droplets, due to either imperfections in the insertion time for each droplet (i.e., the time at which each droplet forms) or velocity fluctuations as each droplet traversed the channel, caused the large and apparently periodic errors seen in Figure 9D. While the procedure of deconvolution of the signal described above is applicable to any sequence of  $\{\alpha_k\}$ , we made two assumptions: (i) the linear speed of the droplets in the channel is constant throughout the channel, and (ii) the spacing between droplets is equal (i.e.,  $\alpha_k = (k - 1)\alpha_0$ ) because microfluidic flow-focusing generates droplets at a constant frequency. Characterizing the more detailed pattern of fluctuation in these two parameters allows us to determine  $\{\alpha_k\}$  and increase S/N, thereby increasing the robustness of the method. A tracking window (e.g., a window that generates light with distinct color or polarization) would be useful to measure the exact sequence of the droplets  $\{\alpha_k\}$  in given positions of the coding region. Alternatively, error correction can be introduced into the sequence itself to improve the robustness of the deconvolution procedure by allowing the receiver to recover from errors due to an incorrect noise threshold. Practical use of this type of multiplexing would require stabilizing the system and enhancing its sensitivity, or developing correction schemes to compensate for errors.

## Conclusions

The microfluidic architecture described here, which combines immiscible fluids flowing in a microchannel with an optical mask that encodes information by selectively transmitting light, is a new example of infochemistry. It relies—at its core—on the very high regularity with which a flow-focusing junction of the sort developed by Stone, Gañán-Calvo, and our group generates droplets.<sup>8,9,15</sup> This regularity is the ultimate “clock” for this system. The flow-focusing junction controlled the ordering of flow of two fluids of differing chemical composition in a single microfluidic channel; the differing chemistry of the fluids—responsible for their differing properties of optical transmission—provided the mechanism to convert light from a single, constant source to an encoded series of optical pulses.

The device translated information encoded as windows in the mask to pulses of light with the following characteristics: (i) The system transmits data at a rate of 40 characters/s (120 Hz, 3 windows per character). This system can transmit a 24-character message in 0.6 s. The tunability of the bit rate could be exploited for lock-in detection. (ii) The system uses multiple properties of light (e.g., intensity, color, and polarization, not all of which are orthogonal in every possible application) to encode information using base- $N$  systems (with  $N > 2$ ). (Phase angle could also be used with a coherent light source, such as a laser, but we have yet explored this parameter.) Such encoding schemes have more information per unit (or window) than binary schemes but generally have the disadvantages of complex implementation and increased potential for quantization error. Error correction schemes for systems with large  $N$  remain to be developed. (iii) The system transmits the same information

reproducibly for a long duration of time. We demonstrated that the system generated indistinguishable signals consisting of eight pulses of light over 4800 times during 80 min of operation. (iv) The microfluidic system does not require large quantities of fluid for prolonged operation. A total volume of 500 mL of liquid would be sufficient to transmit a message at 60 Hz for 100 h. (v) The microfluidic hardware is versatile and reusable: because the message is encoded in the mask, and not in the microfluidic device, the same device can be used to transmit messages of differing lengths and formats (color-based, polarization-based, etc.). In principle, new masks could be made on demand and in the field. Error checking and correction is a crucial part of any scheme for coding, transmitting, receiving and decoding information. We have not focused on this problem here (although we will deal with it in subsequent publications) because we already use a robust form of bit checking: that is, we transmit the same message repetitively. Comparison (and integration) of multiple copies of the same message provides both bit checking and a method of increasing S/N.

Microfluidic devices (especially flow-focusing bubble and droplet generators) are uniquely adaptive systems to use in exploring the integration of chemistry with information technology. The characteristics of microfluidic systems offer the capability to integrate chemistry (such as sensing and reaction kinetics) into the system. In addition, they offer frequencies (currently the maximal frequency of formation of bubbles is  $\sim 100$  kHz<sup>15</sup> and of droplets is  $\sim 10$  kHz<sup>16</sup>) that, although not as fast as electronic circuitry, are remarkable for a hand-held, nonelectronic physical system. This feature will allow future infochemical devices based on these and related methods to combine strategies that are highly developed in electrical and photonic information technology (e.g., checksums and error correction algorithms) with the ability to encode information in multiple physical parameters using chemical and fluidic processes and to generate base- $N$  encoded optical signals.

The system is easy to extend: in this article, we explored encoding schemes that used an optical mask, but additional layers of encoding based on chemistry and physics would be possible in the same architecture using the properties of fluids (i.e., time-independent or time-dependent changes in physical and optical properties of droplets via chemical reactions, mixing, diffusions, or dissociation), properties of the droplet generator (i.e., size, generation frequency, or sequences of droplets), and transmissivity of windows (i.e., colorimetric responses to environmental conditions).

Although it is well suited for exploring the fundamental science of infochemistry, the current system needs further developments and optimization before it can be a practical system for communication. One major challenge is that transmission of messages is short-range. We have demonstrated a resolvable optical signal only over short distances ( $\sim 50$  cm) with the optics we have used. A higher power light source would be required for the reception of signals at long distances.

The current system does not constitute an entirely “chemical” (e.g., nonelectrical) system for communication for several reasons, of which we emphasize four here. (i) It used digital syringe pumps for delivery of the fluids. This reliance on electrical power could be easily eliminated: compressed gas or vacuum could serve to drive flow of fluids through the device.<sup>15,32</sup> (ii) The source of light requires electrical power.

(32) Sia, S. K.; Linder, V.; Parviz, B. A.; Siegel, A.; Whitesides, G. M. *Angew. Chem., Int. Ed.* **2004**, *43*, 498–502.

The current design of this device requires an external source of light; future designs will incorporate chemiluminescent fluids into the microfluidic channel in lieu of an external, electronically powered source. (iii) The detection of signals at high speed (100–1000 Hz) requires sophisticated electronics (i.e., a high-speed camera and/or spectrometer). While the issue of detection is not directly relevant to the focus of this paper on encoding and transmitting signals, it might become important for particular applications. (iv) We fabricated the mask using printers which are electrically driven. Patterned chemistry could, in principle, also be used to create these masks.

Significantly, given the degree to which optical communication has revolutionized the storage and transmission of data, the interplay between light and chemistry demonstrated by this system may offer interesting opportunities for the use of such microfluidic devices and chemistry-based solutions in chemical or molecular computing, provided that appropriate methods to detect, store, and retransmit this information are developed.

### Experimental Section

**Design and Fabrication of the Mask.** The microfluidic channels were prepared using soft lithography.<sup>22,33</sup> The height of the channel was nearly uniform at 150  $\mu\text{m}$ . We sealed a plasma-oxidized polydimethylsiloxane (PDMS) mold to a glass slide (Corning) to prepare the channel system. To prevent wetting to the inner surface of the device by the dispersed phase, the channel was filled with the continuous phase (i.e., aqueous black ink) immediately after the device was sealed. A transparency mask with the desired sequence of optical windows was designed using Clewin (PhoeniX, The Netherlands) and printed by CAD/Art Services (Bandon, OR). The resolution of the photoplotting printer was 20 000 dpi (1.25  $\mu\text{m}$ ). Colored masks were prepared by manually painting windows

with Lumocolor permanent ink (STAEDTLER, pen tip diameter was 0.4 mm). Polarized masks were prepared by aligning polarizing films (Edmund Optics, Barrington, NJ) in the desired orientation underneath each window.

**Microfluidic Flow-Focusing Droplet Generator.** Digital syringe pumps (Harvard Apparatus, model PhD2000) controlled the delivery of the continuous phase (Waterman, aqueous black ink) to the microfluidic device. A pressure-regulating valve connected to a gas cylinder controlled delivery of the dispersed phase (perfluoromethyldecalin (PFMD), 85%, Alfa Aesar). Polyethylene terephthalate (PET) tubing (Becton, Dickinson and Co.) connected the device with the source of the fluid.

**Detection of Light.** A broadband light source (OSRAM GmbH) was used for all experiments. We used an upright microscope (Leica DMRX) and a set of still (Nikon digital camera DXM 1200) and fast video cameras (Phantom V7) to visualize and record movies of the system. The fast video camera captured black/white movies, which were subsequently analyzed by homemade software; the total intensity of the light transmitted by the coding region was measured and plotted using Matlab. The colored signals were captured by imaging the mask onto the fiber-optic imaging input of a high-speed spectrometer (Ocean Optics, HR2000+). The intensity at each wavelength was measured and plotted after the intensity was subtracted from the background using homemade software in Matlab. The Fourier analysis was done in Matlab.

**Acknowledgment.** This material is based upon work supported by DARPA award number W911NF-07-1-0647. A.K.E. was supported by the Ford Foundation. S.W.T. thanks the American Cancer Society for a postdoctoral fellowship.

**Supporting Information Available:** Sample coding schemes for the  $N = 2$  and  $N = 4$  systems, and a movie showing the operation of the device. This material is available free of charge via the Internet at <http://pubs.acs.org>.

JA904788M

(33) Xia, Y. N.; Whitesides, G. M. *Annu. Rev. Mater. Sci.* **1998**, *28*, 153–184.